# Rudhira-mediated microtubule stability controls TGFβ signaling during mouse vascular development.

Divyesh Joshi[1#], Preeti Jindal[1#], Ronak Shetty[1] and Maneesha S. Inamdar[1,2*]

[1]Jawaharlal Nehru Centre for Advanced Scientific Research, Bangalore, India;. [2]Institute for Stem Cell Science and Regenerative Medicine (inStem), Bangalore, India.

# Equal contribution

*Author for correspondence

Email: inamdar@jncasr.ac.in

Tel: +91-080-2208-2818

ORCID: 0000-0002-8243-2821

**Running title:** Rudhira bridges microtubule stability and TGFβ signaling.

**Keywords:** Rudhira; BCAS3; Microtubule cytoskeleton stability; Smad2/3; TGFβ signaling

**Abstract**

The Transforming Growth Factor β (TGFβ) signaling pathway is critical for survival, proliferation, and cell migration, and is tightly regulated during cardiovascular development. Smads, key effectors of TGFβ signaling, are sequestered by microtubules (MTs) and need to be released for pathway function. Independently, TGFβ signaling also stabilizes MTs. Molecular details and the *in vivo* relevance of this cross-regulation remain unclear, understanding which is important in complex biological processes such as cardiovascular development. Here, we use *rudhira/Breast Carcinoma Amplified Sequence 3 (BCAS3)*, a MT-associated, endothelium-restricted and developmentally essential proto-oncogene, as a pivot to decipher cellular mechanisms in bridging TGFβ signaling and MT stability. We show that Rudhira regulates TGFβ signaling *in vivo,* during mouse cardiovascular development, and in endothelial cells in culture. Rudhira-MT association is essential for the activation and release of Smad2/3 from MTs. Consequently, Rudhira depletion attenuates Smad2/3-dependent TGFβ signaling thereby impairing cell migration. Interestingly, Rudhira is also a transcriptional target of Smad2/3-dependent TGFβ signaling essential for TGFβ-induced MT stability. Our study identifies an immediate early physical role and a slower, transcription-dependent role for Rudhira in cytoskeleton- TGFβ signaling crosstalk. These two phases of control could facilitate temporally- and spatially restricted targeting of the cytoskeleton and/or TGFβ signaling in vascular development and disease.

43 **Significance statement**

44 The developmental TGFβ pathway is essential for cell migration, cell-cell communication, adhesion,
45 apoptosis, and matrix remodeling. Dysregulation of TGFβ signaling leads to aberrant vascular
46 patterning and angiogenesis during mouse embryogenesis. Pathway activation involves
47 phosphorylation and nuclear transport of Smads. Microtubules sequester Smads in the cytoplasm,
48 thereby inhibiting TGFβ signaling. Conversely, TGFβ signaling stabilizes microtubules. However, the
49 molecular components involved, and biological relevance of this cross-regulation remain unclear. We
50 show that the oncoprotein Rudhira/BCAS3 facilitates Smad-MT dissociation upon ligand-mediated
51 TGFβ receptor activation. Interestingly, Smad-dependent TGFβ signaling activation enhances rudhira
52 transcription, essential for microtubule stabilization during cardiovascular development. This dual
53 regulation of TGFβ signaling and microtubule stability by Rudhira allows sustained temporal control
54 essential for development, and its dysregulation has pathological outcomes.

55

56

57 **Introduction**

58

59 Cytoskeletal organization and growth factor signaling are mutually dependent and coordinate
60 multiple cellular processes [1]. The multifunctional Transforming growth factor β (TGFβ) pathway
61 regulates cell proliferation, differentiation, survival and migration and is sensitive to cytoskeletal
62 rearrangements [1-3]. Depletion of TGFβ pathway components causes developmental
63 abnormalities often leading to embryonic death [4]. Ligand binding activates the TGFβ receptor,
64 causing receptor-mediated phosphorylation, followed by nuclear translocation of Smad
65 proteins, resulting in transcriptional regulation of target gene expression [5]. Smads, the effectors
66 of the TGFβ pathway, are competitively bound by several proteins and are a hub for regulation
67 of TGFβ signaling and its intersecting pathways [6]. MTs bind to and sequester Smad2/3 and
68 Smad4, thereby negatively regulating TGFβ signaling, which is relieved upon TGFβ stimulation
69 [7]. Conversely, TGFβ signaling stabilizes MTs [8, 9] through an as yet unclear mechanism,
70 suggestive of a feedback loop.

71

72 During development, TGFβ signaling is activated in endothelial cells (ECs) of the remodeling
73 angiogenic endothelium and is critical for vascular development [10]. MT stability is also essential
74 for angiogenic sprouting in ECs [11]. MTs can be stabilized in multiple ways within the cell, initially
75 by RhoA-mDia actin bundling and thereafter by interaction with multi-protein complexes. Serum
76 components, TGFβ and Lysophosphatidic acid (LPA), have been shown to stabilize MTs [8, 12].
77 While LPA stabilizes MTs within 30 min post-stimulation and generically [12], the effect of TGFβ
78 signaling takes at least 2 hours [8] but is more restricted to and essential for endothelial cell
79 function *in vivo*. Slow and restricted induction of MT stability by TGFβ as compared to the more
80 generic and rapid function of LPA suggests a requirement for new transcription/translation which
81 may be developmentally important. However, the molecular mechanisms and biological
82 relevance of cytoskeletal interactions with TGFβ signaling remain elusive. Characterization of
83 tissue-restricted regulators of the ubiquitous MT cytoskeleton may aid in defining its specialized
84 context- dependent functions.

85

86 In this study, we address the role of the MT-interacting protein Rudhira in connecting TGFβ signaling
87 and MT stability. Rudhira associates with MTs and intermediate filaments (IFs), stabilizes MTs and

promotes directional cell migration [11, 13]. *Rudhira* knockout in mouse causes mid-gestation lethality due to aberrant cardiovascular patterning [14]. Transcriptome analysis showed that several processes were deregulated in the *rudhira* knockout, especially, a large number of TGFβ signaling pathway components [14]. This suggests that Rudhira may regulate TGFβ signaling for vascular development.

Here, we show that Rudhira-depleted cells have reduced Smad2/3 activation during mouse embryonic development, indicating that Rudhira is a positive regulator of TGFβ signaling. We demonstrate that Rudhira facilitates TGFβ-mediated release of Smad2/3 from MTs. Further, TGFβ signaling stabilizes MTs by inducing transcription, in a Rudhira-dependent manner. Thus, Rudhira bridges TGFβ signaling and MT stability, required for cardiovascular development. Ectopic and aberrant Rudhira expression is seen in several carcinomas and positively correlates with tumor metastatic potential [15-17]. Hence our study will aid understanding of TGFβ signaling and suggest novel ways to regulate it in development and disease.

## Results

### Rudhira depletion attenuates Smad2/3-dependent TGFβ signaling *in vivo* and *in vitro*

*Rudhira* is an essential gene, critical for mouse cardio-vascular development [14]. Ubiquitous (*rudh*$^{-/-}$) or endothelial (*rudh*$^{CKO}$) knockout of *rudhira* results in angiogenic defects and mid-gestation embryonic lethality [14]. Transcripts of several components of the TGFβ pathway are deregulated upon Rudhira depletion and the knockout phenocopies mutants of several TGFβ pathway components, whose primary phenotype is in the cardiovascular system [10]. Hence, we characterized the role of Rudhira in TGFβ signaling. Analysis of the molecular interaction, reaction and relation networks by KEGG pathway mapping indicated that multiple components of the TGFβ pathway were deregulated in the absence of Rudhira, affecting several processes important for cardiovascular development (Fig. 1A). To validate this, we used non-silencing (NS) control and rudhira knockdown (KD) saphenous vein endothelial cell lines (SVEC) as described before (Fig S1A, B) [14]. To test the pathway regulation at the level of receptors, we analysed transcript and basal as well as active protein levels. While we observed some reduction in transcript levels of

119 *tgfbrI* and *tgfbrII* (Fig. S2A), the basal and active protein levels of TGFβRI remained unchanged in
120 KD cells (Fig. S2B). Interestingly, a constitutively active form of TGFβRI (TGFβRIT204D), expressed
121 under the CMV promoter, was also suppressed in Rudhira KD (overexpression achieved in NS ~200
122 folds while in KD ~80 folds) (Fig. S2C). TGFBR1 protein has a short half-life, while the mRNA is
123 relatively stable [18]. Reduced amount of relatively stable RNA may be sufficient to produce
124 adequate protein levels. These increased levels of active TGFβRI in KD were unable to restore
125 Smad2 phosphorylation, unlike NS controls, which showed a clear increase (Fig. 1B). While
126 important to note that Rudhira or its loss may regulate *tgfbr* transcript levels, these results support
127 a receptor-independent role of Rudhira in regulating TGFβ pathway.
128
129 To probe further into the molecular mechanism by which Rudhira controls TGFβ signaling, we used
130 *rudhira* knockout mice and the KD endothelial cell line. Upon TGFβ-stimulation ECs in culture showed
131 reduced Smad2 activation in the KD as compared to NS control (Fig. 1C). Further, qRT-PCR analysis
132 showed that transcript levels of Smad2/3 targets, namely *mmp9* and *pai1*, did not increase
133 significantly in KD, whereas NS control showed >2-fold increase for both (Fig. 1D). Expectedly, partial
134 restoration of Rudhira level in KD cells restored Smad2 activation and target gene expression (Fig.
135 1C, D). The canonical TGFβ pathway also responds to BMP4 activation. However, upon stimulation
136 with BMP4 there was no significant difference in the levels of pSmad1/5/8 between NS and KD (Fig.
137 S2D). These data indicate that Rudhira is required for TGFβ-dependent Smad2 phosphorylation and
138 pathway activation.
139
140 Endothelial depletion of Rudhira (*rudh*$^{CKO}$) is sufficient to cause vascular defects [14] and functional
141 TGFβ signaling is essential for vascular development [19]. Expectedly, *rudh*$^{CKO}$ embryos showed a
142 concomitant loss of pSmad2/3 in the embryonic endocardium (Fig. 1E, E'), without affecting the
143 total Smad2/3 level (Fig. S2E, E'). Thus, Rudhira regulates TGFβ signaling in a Smad2/3-dependent
144 manner *in vivo*, which is essential for angiogenesis and endothelial cell migration during cardio-
145 vascular development.
146
147 **Rudhira is required for TGFβ mediated cell migration**
148 As Rudhira is essential for cell migration, we tested the effect of altered TGFβ pathway activity in
149 Rudhira KD endothelial cells (SVEC) in a transwell migration assay. We also validated our results in
150 HEK293 cells as these allow a high efficiency of transfection and Rudhira overexpression, for

151 migration assays. TGFβ addition did not enhance migration in *rudhira* knockdown (KD) cells as
152 compared to controls (NS and rescued KD) (Fig. 2A). In addition, ectopic Rudhira expression in
153 HEK293 cells caused increase in migration rate as compared to the control, consistent with our
154 earlier study [13] (Fig. 2B,C).
155
156 TGFβ supplementation of Rudhira overexpressing cells dramatically enhanced the rate of cell
157 migration (~2.6 fold), suggesting a direct correlation between Rudhira levels and pathway
158 function (Fig. 1C, D). Serum contains TGFβ in a concentration range of 10-40 ng/ml [20] and
159 we used 5% FBS with or without additional TGFβ in the transwell migration assay, since purified
160 TGFβ alone is unable to induce migration. The ratio of increase in migration rates with or without
161 exogenous TGFβ addition was similar in both the control and Rudhira-overexpressing cells (~1.5
162 fold). Interestingly, TGFβ pathway-inhibition by SB431542 (SB) restored the effect of Rudhira
163 overexpression (enhancement in cell migration rate) to control levels (Fig. 2B, S3A) suggesting
164 that Rudhira function is regulated by the TGFβ pathway downstream of receptor activation. In
165 addition to the multiple molecular pathways that function in concert to control cell migration [21],
166 our data support a role for Rudhira in TGFβ-dependent cell migration.
167
168 **Rudhira regulates TGFβ signaling by promoting the release of Smad2/3 from MTs**
169 Since Rudhira localizes to the cytoskeletal components, namely microtubules and intermediate
170 filaments [13], we hypothesized that it regulates TGFβ signaling at the cytoskeleton. However, we
171 could not detect any interaction between Rudhira and Smad2/3 under the conditions tested (Fig.
172 3A), suggesting that the effect on the pathway may be indirect, possibly through MTs. TGFβ
173 signaling is controlled at multiple levels, including cytoskeletal regulation at MTs, which interact
174 with and sequester Smad2/3 thereby inhibiting the TGFβ pathway [7]. TGFβ stimulation releases
175 Smads from MT sequestration in multiple cell types including endothelial cells, facilitating its
176 activation and nuclear translocation [7]. Expectedly, TGFβ stimulation in ECs (confirmed by increase
177 in pSmad2 levels) reduced Smad-MT binding as seen by co-immunoprecipitation for β-Tubulin
178 and immunoblotting for Smad2 (Fig. 3B).
179
180 To assess whether Rudhira is required for TGFβ-dependent release of Smad from MTs, we tested
181 for β-Tubulin and Smad interaction upon TGFβ stimulation in NS and KD cells by performing *in situ*
182 Proximity Ligation assay (PLA) [22]. While NS cells showed reduced Smad-MT interaction, KD cells

183 retained Smad-MT interaction even upon TGFβ stimulation in multiple KD cell lines (Fig. 3C, Fig. S3B).
184 Interestingly, TGFβ stimulation resulted in an increase in Rudhira-MT association in wild type
185 cells, detected by colocalization (Fig. 3D) and confirmed by PLA (Fig. 3E). Thus TGFβ-stimulated
186 Rudhira-MT association makes MTs unavailable for Smad binding. However, MTs are abundant and
187 present as subsets, differing in their Tubulin isotype and isoform composition, post translational
188 modifications (PTMs) and stability [23], which may also govern their interactions with other
189 molecules. It is unlikely that Rudhira binds to all MTs present. Also, it is likely that only a subset of
190 MTs may bind and sequester Smads.
191

192 ***Rudhira* is a transcriptional target of TGFβ signaling and is essential for MT stability**

193 The TGFβ pathway is auto-regulatory, due to which several pathway components are induced
194 or inhibited [24, 25]. The *rudhira* promoter harbors putative Smad-binding elements (SBEs) (Fig.4A).
195 It also harbors putative binding sites of major TGFβ pathway regulated transcription factors (TFBS)
196 (Fig.S4A, Table S2). Expectedly, TGFβ stimulation increased *rudhira* mRNA and protein levels (Fig. 4B,
197 C, D). Knockdown of *smad2* or *smad3* resulted in significant reduction of Rudhira levels, indicating
198 that *rudhira* is a Smad2/3-dependent TGFβ target (Fig. 4E). Blocking transcription with
199 Actinomycin D (AcD) or translation using Cycloheximide (CHX) prevented increase in *rudhira*
200 levels upon TGFβ stimulation, confirming that *rudhira* is a transcriptional target of the Smad2/3-
201 dependent TGFβ pathway (Fig. 5A, S4B). However, additional investigation is required to confirm
202 whether *rudhira* is a direct target of Smad2/3-dependent TGFβ pathway.
203

204 Rudhira and TGFβ signaling, both can induce MT stabilization [8, 11]. Although the mechanism
205 is unclear, PTMs and/or transcription may control TGFβ-induced MT stability [8]. Since *in vivo*
206 studies indicated that *rudhira* deletion severely affects the TGFβ pathway [11], we tested whether
207 TGFβ- induced transcription is required for MT stability. TGFβ stimulation results in a slow
208 enhancement of MT stability over a period of several hours, allowing sufficient time for
209 transcriptional regulation [8]. Interestingly, we find that blocking transcription or translation,
210 prevented TGFβ-dependent MT stabilization, as detected by Glu-tubulin levels (Fig. 5A, S4B),
211 correlating well with Rudhira levels and validated by increased sensitivity to Nocodazole-mediated
212 MT depolymerization (Fig. 5B). These data show that TGFβ induced MT stability is transcription-
213 dependent.
214

215 **TGFβ signaling stabilizes MTs in a Rudhira-dependent manner**

216 Since *rudhira* transcription is dependent on TGFβ signaling and Rudhira is required for MT stability,
217 we further tested whether TGFβ-induced MT stability is Rudhira-dependent. Serum starvation
218 resulted in low detectable levels of Glu-tubulin in NS and KD cells (Fig. 5C). Stimulation with
219 TGFβ or serum led to increased Glu-tubulin level in NS but not in KD cells showing that TGFβ-
220 induced MT stability is dependent on Rudhira (Fig. 5C, S4C). To test whether Rudhira stabilizes
221 MTs *in vivo* also, we analyzed the effect of loss of Rudhira on MT stability in the developing
222 endocardium. Interestingly, along with reduced pSmads levels observed earlier (Fig. 1E, E'), we found
223 that Glu-tubulin positive stable MTs were fewer in *rudh*$^{CKO}$ embryonic endocardium (Fig. 5D),
224 supporting a role of Rudhira in regulation of TGFβ signaling and MT stability during cardiovascular
225 development. Combined, our study suggests that Rudhira primarily affects MTs to modulate
226 their Smad-binding property and downstream TGFβ signaling. Consequently, Smad2/3-dependent
227 TGFβ signaling induces *rudhira* transcription leading to MT stabilization essential for cardiovascular
228 remodeling during development (Fig. 5E).

229

230

231

232 **Discussion**

233 Growth factor signaling and cytoskeletal remodeling are mutually dependent processes that
234 require complex context-dependent molecular crosstalk [1]. Specifically, the developmentally
235 essential, tissue-restricted TGFβ signaling pathway, regulates and is regulated by the MT
236 cytoskeleton. However, the underlying molecular mechanism and *in vivo* relevance of this cross-
237 regulation remain elusive. In this study, we probed the role of Rudhira in the cytoskeletal control
238 of TGFβ signaling and, in turn, its effect on MT properties. Our study identifies a dual role of
239 Rudhira during vascular development- as a MT-mediated regulator and a transcriptional target
240 of TGFβ signaling required for MT stability.

241

242 While several processes important for cardiovascular development were deregulated in
243 *rudhira*$^{-/-}$ embryos, the TGFβ pathway was primarily affected [14]. TGFβ signaling is a complex
244 pathway and is regulated at multiple levels by various feedback loops. One of the complicated yet
245 delicate feedback circuits is the regulation of receptor levels and activity [25]. Rudhira depletion
246 reduces transcript level without altering basal and active protein level of TGFBRI. This disparity in the
247 transcript and protein level may arise from the fact that while the *tgfbr* transcript is very stable, the
248 protein is quite unstable, and lower transcript levels may still be sufficient for generating adequate
249 protein levels. Such a phenomenon is not unusual, particularly for membrane proteins, where mRNA
250 levels may not correlate with protein levels. Rudhira, in a manner not yet understood, may also be
251 a part of a broader feedback pathway as it further negatively regulates levels of TGFβ pathway
252 inhibitors such as Smurfs and inhibitory Smads, Smad6 and Smad7 (Fig. S3C). This control on
253 inhibitors is seen even in the absence of TGFβ stimulation, suggesting that additional regulatory
254 mechanisms may operate.

255

256 TGFβ signaling and Rudhira promote cell migration in a synergistic and inter-dependent manner.
257 Mechanistically, Rudhira promotes TGFβ-dependent release of Smads from MTs likely due to
258 increased Rudhira-MT association. This could allow pathway activation and result in enhanced cell
259 migration. Additional, confounding factors downstream of the autoregulatory TGFβ pathway or
260 pathway targets, as described above, may also contribute to Rudhira dependent cell migration in
261 response to TGFβ. Converse regulation of Rudhira-MT and Smad-MT interaction is indicative of
262 probable competition between Smads and Rudhira for MT binding, which merits further
263 investigation. Binding of Rudhira to MTs may also alter them in a way that makes MTs unavailable

264 for Smad binding. This study supports the hypothesis that dissociation of Smads from MTs is essential
265 for Smad activation. In addition, though MTs are ubiquitously and abundantly present, our data
266 suggest that only a few MTs participate in Smad sequestration. This is in concordance to our
267 earlier study which shows that Rudhira associates preferentially with stable MTs [11].
268
269 The TGFβ signaling pathway is autoregulatory and many of its components are also targets of the
270 pathway [24]. The *rudhira* promoter harbors Smad Binding Elements (SBEs). We show that Rudhira,
271 in addition to being a regulator of the TGFβ pathway, is also a transcriptional target. However,
272 further analysis is required to identify the specific mechanisms by which Smad-dependent, TGFβ-
273 induced, *rudhira* transcription is regulated during development.
274
275 *Rudhira* expression is tightly regulated and restricted to the remodeling endothelium
276 during development [14]. Mechanistically, Rudhira promotes MT stability for angiogenic
277 remodeling [11]. Independent studies show that TGFβ signaling, and MT reorganization are
278 essential for cardiovascular development [26-28]. Deletion of *smad2/3* or *tubulins* leads to
279 embryonic lethality with severely defective embryonic and extra-embryonic vasculature [29].
280 However, the role of MT stability for angiogenic sprouting *in vivo* and the underlying molecular
281 mechanisms remain elusive. Our study suggests that endothelial cytoskeleton remodeling by
282 Rudhira and activation of TGFβ signaling during cardiovascular development are inter-dependent
283 and cross-regulated. TGFβ signaling may lead to restricted induction of MT stability by inducing
284 the expression of MT-stabilizing developmentally regulated proteins like Rudhira. Additional
285 cytoskeletal components such as Vimentin that interacts with Rudhira, and is also a target of TGFβ
286 signaling, are likely to be involved [11, 13]. Our analysis will help gain better insight into cellular
287 processes such as migration, which require maintenance of cytoskeletal stability and active
288 signaling for extended periods. An added advantage will be the ability to decipher deregulated
289 migration such as in tumor metastasis. While targeting MT-Smad interaction would allow
290 regulation of the TGFβ pathway, the ubiquitous nature of these molecules is likely to result
291 in widespread and possibly undesirable effects of therapeutic intervention. Rudhira expression,
292 being more restricted, could provide a suitable target to regulate developmental and pathological
293 TGFβ signaling.
294
295

296 **Materials and methods**

297

298 **Animal experiments**

299 Animal experiments were performed as mentioned earlier [14]. All animal experimental protocols
300 were approved by the Institutional Animal Ethics Committee (IAEC) of JNCASR (Project number
301 MSI006. All animals were maintained, and experiments were performed according to the guidelines
302 of the animal ethics committee of JNCASR. *Rudhira* floxed mice and conditional knockout mice (*Tek-*
303 *Cre* mediated endothelial deletion, *rudhira*$^{flox/flox}$*; TekCre*$^{+}$, abbreviated to *rudh*$^{CKO}$) were validated by
304 genotyping.

305

306 **Cell culture, transfections, and small molecule treatments**

307 Cell line sources and generation is reported elsewhere [14]. In brief, *rudhira* shRNA vectors (715,
308 716), and scrambled (non- silencing) control vector (TR30015) (Origene, USA) were microporated
309 into SVEC (mouse endothelial cell line) and selected for stable line generation. Control cell line is
310 referred to as 'NS' and *rudhira* knockdown as 'KD'. For Rudhira overexpression and rescue line, the
311 plasmid constructs used were GFP-2A-GFP and Rudh-2A-GFP which are described elsewhere [13].
312 Constitutively active TGFβRI (pcDNA3-ALK5 T204D, 80877) was purchased from addgene for
313 transfection of SVEC NS and KD cells. Control and shRNA vectors for s*mad2* or *smad3* knockdown)
314 were purchased from ShRNA Resource Centre (Department of Microbiology and Cell Biology, Indian
315 Institute of Science, Bangalore, India) and were from the SIGMA Library of shRNAs for Human gene
316 products. The shRNAs were transfected in HEK293T cells and selected in 1 µg/ml Puromycin for 7
317 days. Details of the oligonucleotide sequence of the shRNAs are provided in Supplementary Table S3.
318 HEK293, HEK293T cellswere transfected using Calcium Phosphate method while SVEC cells were
319 transfected using Lipofectamine 2000 (ThermoFisher Scientific, USA). All small molecules were from
320 Sigma Chemical Co., USA, and treatments were performed in DMEM, unless otherwise indicated.
321 Cells were washed three times in PBS and serum starved for 12h. Thereafter, cells were kept
322 untreated or treated with 10 ng/ml of TGFβ (Fig. 1C) or BMP4 (Fig. S2D) for 2 h and then taken for
323 immunoblotting. For gene expression analysis, cells were induced with 10 ng/ml of TGFβ for 24 to 48
324 h (Figs. 1D, 4B, C, D). SB431542 was used at a concentration of 10 µM, as indicated (Fig. 2A, B and

325 S3A). For Transwell migration assays, small molecule dilutions were prepared in 5% FBS containing
326 DMEM (Fig. 2A, B). For interaction studies cells were serum starved for 12h and thereafter kept
327 untreated or treated with 10 ng/ml of TGFβ or 10% FBS for 2 h and then taken for PLA,
328 immunostaining or western blotting, as desired (Fig. 3). For TGFβ-dependent *rudhira* transcription
329 and MT stability assays, cells were serum starved for 48h in serum-free medium (SFM) containing 5
330 mg/ml BSA and 20mM HEPES (pH 7.4) in DMEM. Thereafter, various treatments were performed for
331 7h (Fig. 5A, B, C). TGFβ (10 ng/ml), Actinomycin D (AcD, 10 µM), Cycloheximide (50 µg/ml) were
332 diluted in SFM.
333

334 **Quantitative RT-PCR (qRT-PCR)**

335 RNA was isolated using TRIzol reagent (Invitrogen). Reverse transcription was performed using 2 µg
336 of DNase treated RNA and Superscript II (Invitrogen, Carlsbad, CA) according to manufacturer's
337 instructions. Quantitative RT-PCR (qRT-PCR) was carried out using EvaGreen (BIO-RAD, CA) in Biorad-
338 CFX96 Thermal cycler (BIO-RAD, CA). Details of primers used are provided in Supplementary Table
339 S1.
340

341 **Immunostaining, Immunohistochemistry, Fluorescence Microscopy and Analysis**

342 Yolk sac or embryos dissected at E10.5 were fixed in 4% paraformaldehyde and processed for
343 Cryosectioning (embryos) and immunostaining using standard procedures. Control and knockout
344 embryos were identified by embryonic tail genotyping. Cells were fixed in 4% paraformaldehyde at
345 room temperature or 100% methanol at -20 ˚C and processed for immunostaining using standard
346 procedures [30]. Primary antibodies used were against PECAM1 (CD31) (BD Biosciences, USA),
347 Rudhira, Smad2/3, pSmad2, pSmad2/3 (Cell Signaling Technology), β-Tubulin (DSHB, Iowa), Glu-
348 Tubulin (Abcam), GFP (Invitrogen). Secondary antibodies were conjugated with Alexa-Fluor 488 or
349 Alexa-Fluor 568 or Alexa-Fluor 633 (Molecular Probes). Bright field and phase contrast microscopy
350 were performed using an inverted (IX70, Olympus) microscope. Confocal microscope, LSM 880 with
351 airy scan, Zeiss, was used for fluorescence microscopy. All images in a set were adjusted equally for
352 brightness and contrast using Adobe Photoshop CS2, where required.
353

354 **Immunoblot analysis and co-immunoprecipitation**

355 50 µg whole cell lysate was used for western blot analysis by standard protocols. Blots were cut into
356 strips and incubated with primary antibodies as indicated: Smad2/3, pSmad2, Smad1/5/8,
357 pSmad1/5/8 (Cell Signaling Technology), GAPDH (Sigma Chemical Co., USA), Glu-Tubulin, Ubiquitin,
358 TGFβRI, pTGFβRI (Abcam, USA), β- Tubulin (DSHB, Iowa), Rudhira (Bethyl Labs, USA). HRP conjugated
359 secondary antibodies against appropriate species were used and signal developed by using Clarity
360 Western ECL substrate (Biorad, USA). For co-immunoprecipitation, 500 µg whole cell lysate and 2 µg
361 of the desired antibody were used. Complexes were captured on Protein G-Agarose beads and
362 analyzed by immunoblotting.
363

364 **Transwell migration assay**

365 The assays and quantitation were carried out as mentioned earlier [13]. Briefly, 24 h after
366 transfection with desired plasmid vectors, cells were serum-starved for 12 h and 20000 HEK cells or
367 40000 SVEC were plated onto the upper chamber of the transwell filter inserts with 8 µm pore size,
368 24-well format (Costar, USA). 10% FBS containing medium (with desired small molecules) was added
369 to the lower chamber to serve as a chemo-attractant. After 24 h, cells were fixed in 4%
370 paraformaldehyde for 10 min at room temperature. Cells on the top of the filter were removed using
371 a cotton swab. Cells that had migrated to the bottom were fixed and stained with 0.5% crystal violet
372 for 10 min at room temperature. The dye was extractedin methanol and absorbance measured
373 spectrophotometrically at 570 nm.
374

375 ***In situ* Proximity Ligation Assay (PLA or Duolink assay)**

376 *In situ* PLA (Proximity Ligation Assay) reaction was performed on SVEC cell lines. The cells were
377 cultured, fixed, permeabilised and stained with primary antibodies for Smad2/3, β-Tubulin or
378 Rudhira, as desired. Thereafter, the protocol for PLA as recommended by manufacturer (Duolink,
379 USA) was followed. Post PLA, nuclei were counterstained with DAPI.
380

381 **Rudhira promoter *in silico* analysis**

382 Smad-binding elements or motifs (SBEs) and other transcription factor binding sites (TFBS) were

identified from experimental studies, available in JASPAR database (https://jaspar.genereg.net/). PSCAN software (http://159.149.160.88/pscan) was used for motif scanning in mouse and human *rudhira/BCAS3* gene promoters (1 kb sequence upstream of the transcription start site) using matrices obtained from JASPAR bioinformatics tool, as indicated. (Supplementary Table S2).

**Quantification and Statistical analyses**

Statistical analyses were performed using One Way ANOVA in the Data Analysis package in Microsoft Excel, and two-way ANOVA and one-sample t-test in GraphPad Prism. $p<0.05$ was considered significant.

**Acknowledgements**

We thank Aksah Sam for maintaining mouse stocks; Developmental Studies Hybridoma Bank, University of Iowa, USA for some antibodies; JNCASR Imaging facility, JNCASR Animal Facility, NCBS Animal facility for access and Inamdar laboratory members for fruitful discussions. This work was funded by grants from the Department of Biotechnology, Government of India (Sanction no. BT/PR11246/BRB/10/644/2008 dated 29.09.2009) the Wellcome Trust, UK (094879/B/10/Z) and intramural funds from Jawaharlal Nehru Centre for Advanced Scientific Research, India.

**Author Contributions**

MSI conceived of the project and directed the work. DJ, PJ, RS, MSI performed and analyzed all the experiments. DJ, PJ, MSI wrote the manuscript. Authors have no competing interests.

405 **References**

406


407 1. Tzima, E., *Role of small GTPases in endothelial cytoskeletal dynamics and the shear stress response.*
408 Circ Res, 2006. **98**(2): p. 176-85.
409 2. Guo, X. and X.F. Wang, *Signaling cross-talk between TGF-beta/BMP and other pathways.* Cell Res,
410 2009. **19**(1): p. 71-88.
411 3. Moustakas, A. and C.H. Heldin, *Dynamic control of TGF-beta signaling and its links to the cytoskeleton.*
412 FEBS Lett, 2008. **582**(14): p. 2051-65.
413 4. Lebrin, F., et al., *TGF-beta receptor function in the endothelium.* Cardiovasc Res, 2005. **65**(3): p. 599-
414 608.
415 5. Hata, A. and Y.G. Chen, *TGF-beta Signaling from Receptors to Smads.* Cold Spring Harb Perspect Biol,
416 2016. **8**(9).
417 6. Massague, J., *TGFbeta in Cancer.* Cell, 2008. **134**(2): p. 215-30.
418 7. Dong, C., et al., *Microtubule binding to Smads may regulate TGF beta activity.* Mol Cell, 2000. **5**(1): p.
419 27-34.
420 8. Gundersen, G.G., I. Kim, and C.J. Chapin, *Induction of stable microtubules in 3T3 fibroblasts by TGF-*
421 *beta and serum.* J Cell Sci, 1994. **107 ( Pt 3)**: p. 645-59.
422 9. You, E., et al., *Dynein-mediated nuclear translocation of yes-associated protein through microtubule*
423 *acetylation controls fibroblast activation.* Cell Mol Life Sci, 2020. **77**(20): p. 4143-4161.
424 10. Goumans, M.J., Z. Liu, and P. ten Dijke, *TGF-beta signaling in vascular biology and dysfunction.* Cell
425 Res, 2009. **19**(1): p. 116-27.
426 11. Joshi, D. and M.S. Inamdar, *Rudhira/BCAS3 couples microtubules and intermediate filaments to*
427 *promote cell migration for angiogenic remodeling.* Mol Biol Cell, 2019. **30**(12): p. 1437-1450.
428 12. Cook, T.A., T. Nagasaki, and G.G. Gundersen, *Rho guanosine triphosphatase mediates the selective*
429 *stabilization of microtubules induced by lysophosphatidic acid.* J Cell Biol, 1998. **141**(1): p. 175-85.
430 13. Jain, M., et al., *Rudhira/BCAS3 is a cytoskeletal protein that controls Cdc42 activation and directional*
431 *cell migration during angiogenesis.* Exp Cell Res, 2012. **318**(6): p. 753-67.
432 14. Shetty, R., et al., *Rudhira/BCAS3 is essential for mouse development and cardiovascular patterning.*
433 Sci Rep, 2018. **8**(1): p. 5632.
434 15. Siva, K., et al., *Human BCAS3 expression in embryonic stem cells and vascular precursors suggests a*
435 *role in human embryogenesis and tumor angiogenesis.* PLoS One, 2007. **2**(11): p. e1202.
436 16. Barlund, M., et al., *Cloning of BCAS3 (17q23) and BCAS4 (20q13) genes that undergo amplification,*
437 *overexpression, and fusion in breast cancer.* Genes Chromosomes Cancer, 2002. **35**(4): p. 311-7.
438 17. Gururaj, A.E., et al., *MTA1, a transcriptional activator of breast cancer amplified sequence 3.* Proc Natl
439 Acad Sci U S A, 2006. **103**(17): p. 6670-5.
440 18. Vizan, P., et al., *Controlling long-term signaling: receptor dynamics determine attenuation and*
441 *refractory behavior of the TGF-beta pathway.* Sci Signal, 2013. **6**(305): p. ra106.
442 19. Goumans, M.J. and C. Mummery, *Functional analysis of the TGFbeta receptor/Smad pathway through*
443 *gene ablation in mice.* Int J Dev Biol, 2000. **44**(3): p. 253-65.
444 20. Nockowski, P., et al., *Serum concentrations of transforming growth factor beta 1 in patients with*
445 *psoriasis vulgaris.* Acta Dermatovenerol Croat, 2004. **12**(1): p. 2-6.
446 21. Devreotes, P. and A.R. Horwitz, *Signaling networks that regulate cell migration.* Cold Spring Harb
447 Perspect Biol, 2015. **7**(8): p. a005959.
448 22. Bagchi, S., R. Fredriksson, and A. Wallen-Mackenzie, *In Situ Proximity Ligation Assay (PLA).* Methods
449 Mol Biol, 2015. **1318**: p. 149-59.
450 23. Janke, C., *The tubulin code: molecular components, readout mechanisms, and functions.* J Cell Biol,
451 2014. **206**(4): p. 461-72.

452 24. Miyazono, K., *Positive and negative regulation of TGF-beta signaling.* J Cell Sci, 2000. **113 ( Pt 7)**: p.
453 1101-9.
454 25. Yan, X., X. Xiong, and Y.G. Chen, *Feedback regulation of TGF-beta signaling.* Acta Biochim Biophys Sin
455 (Shanghai), 2018. **50**(1): p. 37-50.
456 26. Ferrari, G., et al., *Transforming growth factor-beta 1 (TGF-beta1) induces angiogenesis through*
457 *vascular endothelial growth factor (VEGF)-mediated apoptosis.* J Cell Physiol, 2009. **219**(2): p. 449-58.
458 27. Martin, M., et al., *Control of endothelial cell polarity and sprouting angiogenesis by non-centrosomal*
459 *microtubules.* Elife, 2018. **7**.
460 28. Bayless, K.J. and G.A. Johnson, *Role of the cytoskeleton in formation and maintenance of angiogenic*
461 *sprouts.* J Vasc Res, 2011. **48**(5): p. 369-85.
462 29. Itoh, F., et al., *Smad2/Smad3 in endothelium is indispensable for vascular stability via S1PR1 and N-*
463 *cadherin expressions.* Blood, 2012. **119**(22): p. 5320-8.
464 30. Schlaeger, T.M., et al., *Vascular endothelial cell lineage-specific promoter in transgenic mice.*
465 Development, 1995. **121**(4): p. 1089-98.
466

467 **Figures**

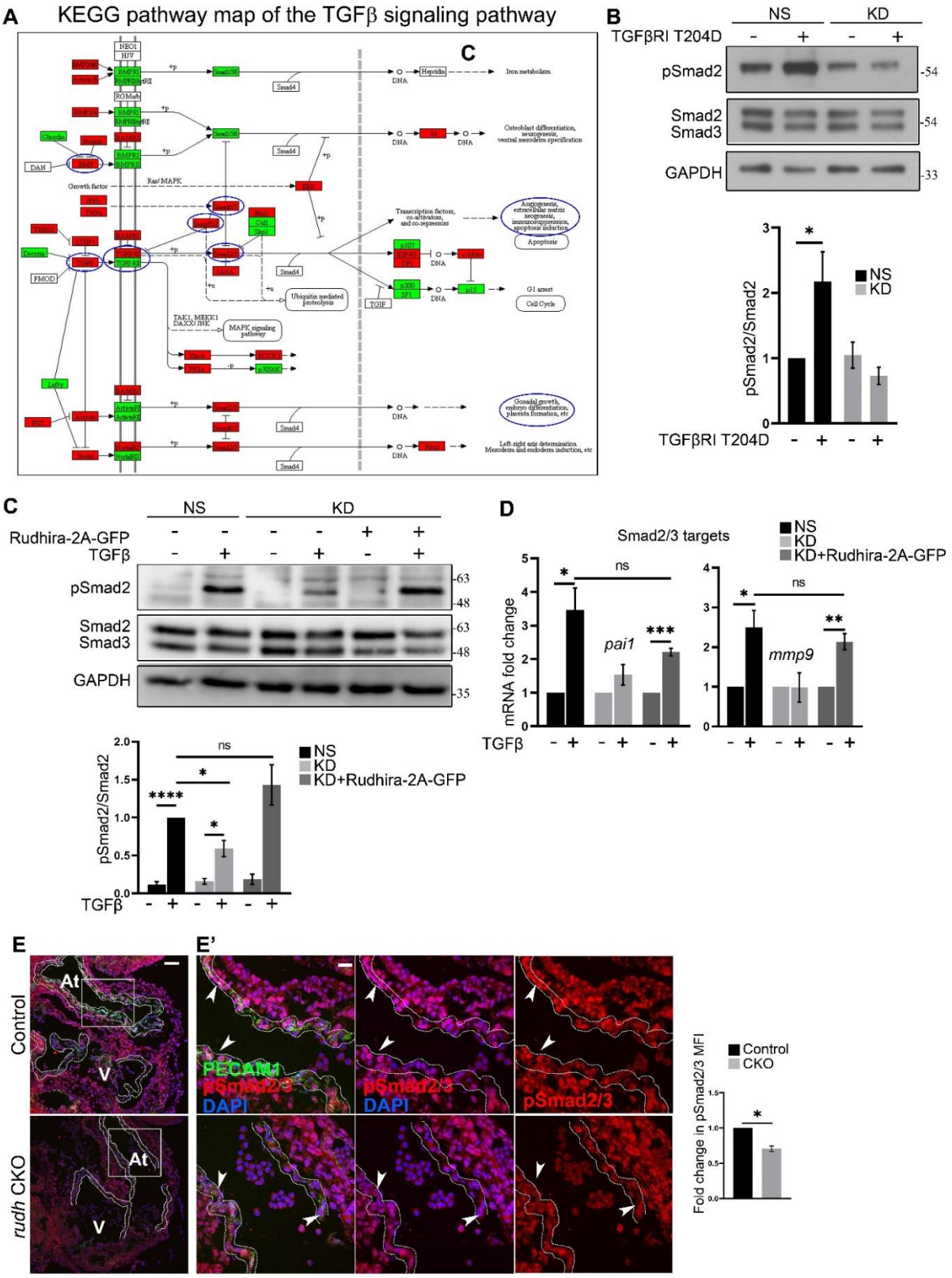


**Figure 1**

468

469

470 **Fig. 1. Rudhira depletion deregulates developmental endothelial TGFβ signaling.** (A) KEGG pathway
471 map indicating TGFβ pathway genes from KEGG database that are deregulated upon *rudhira*
472 depletion in mouse embryonic yolk sac, based on [14]. Genes were mapped based on fold change
473 in *rudhira*$^{-/-}$ yolk sacs in comparison to control to understand pathway regulation. Green:
474 downregulated, Red: upregulated. Blue circles indicate affected genes or processes known to be
475 affected upon Rudhira depletion, from earlier studies. (B) NS and KD SVEC cells, transfected with
476 constitutively active TGFβRI for 24h, were analyzed for Smad2 phosphorylation by Immunoblotting.
477 Graph shows the quantitation of pSmad2/Smad2 levels (N= 3 independent experiments). (C, D)
478 Control (NS), *rudhira* knockdown (KD) and rescued KD (KD + Rudhira-2A-GFP) cells were kept
479 untreated or treated with TGFβ and used for various assays, as indicated. (C) Immunoblot for
480 Smad2/3 and pSmad2. Graph shows the quantitation of pSmad2/Smad2 levels (N= 3 independent
481 experiments). (D) qRT-PCR analysis of *mmp9* and *pai1*, known Smad2/3 targets in ECs (N= 3
482 independent experiments). (E, E') Immunostaining for phosphorylated Smad2/3 in control and
483 *rudhira* conditional knockout *(rudh*$^{CKO}$*)* embryos at E10.5. Boxed region in the embryonic heart in (E)
484 marking the endocardium and the myocardium are magnified in (E') (N= 3 embryos for each
485 genotype). White dotted line indicates the endocardium. Graph shows the quantitation of pSmad2/3
486 levels (N= 3 independent experiments). Statistical analysis was performed using two-way ANOVA
487 .(A, B, C, D) and student's t-test (E). Error bars indicate standard error of mean (SEM). *$p<0.05$,
488 **$p<0.01$, ***$p<0.001$. Scale bar: (E) 100 µm; (E') 20 µm.

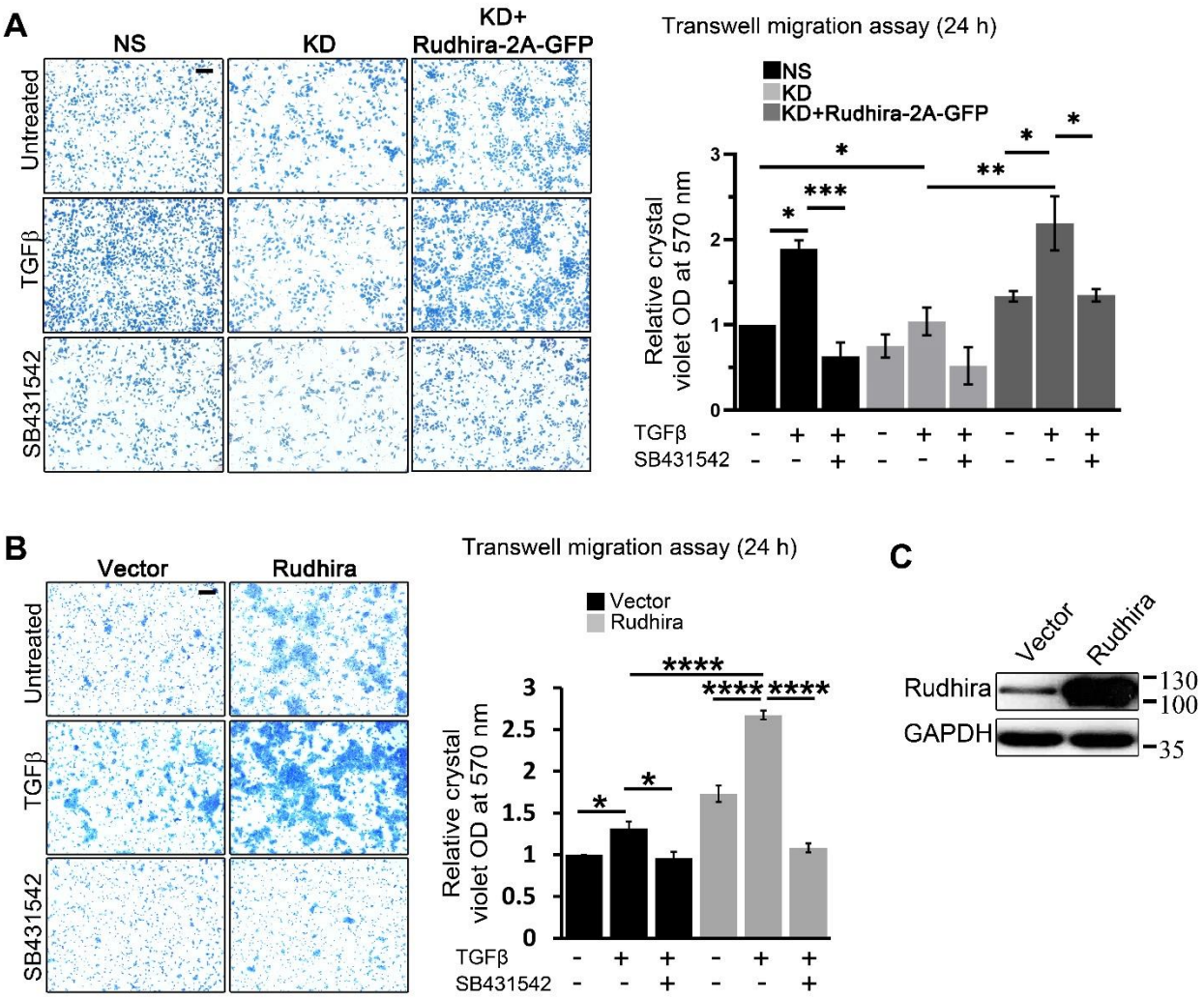


# Figure 2

**Fig. 2. Rudhira functions downstream of TGFβ receptor activation to promote TGFβ-dependent cell migration.** (A) Control (NS), *rudhira* knockdown (KD) and rescued KD (KD + Rudhira-2A-GFP) cells were analyzed for migration rates with or without TGFβ using a transwell migration assay. Graph shows the extent of cell migration as measured by crystal violet absorbance (N= 3 independent experiments). (B, C) HEK293 cells transfected with vector alone or Rudhira were analyzed for migration rates using a transwell migration assay in various conditions, as indicated. Graph shows the extent of cell migration as measured by crystal violet absorbance (N= 3 independent experiments). Statistical analysis was performed using one-way ANOVA. Error bars indicate SEM. Scale bar: (A, B) 100 µm. *p<0.05, **p<0.01, ***p<0.001.

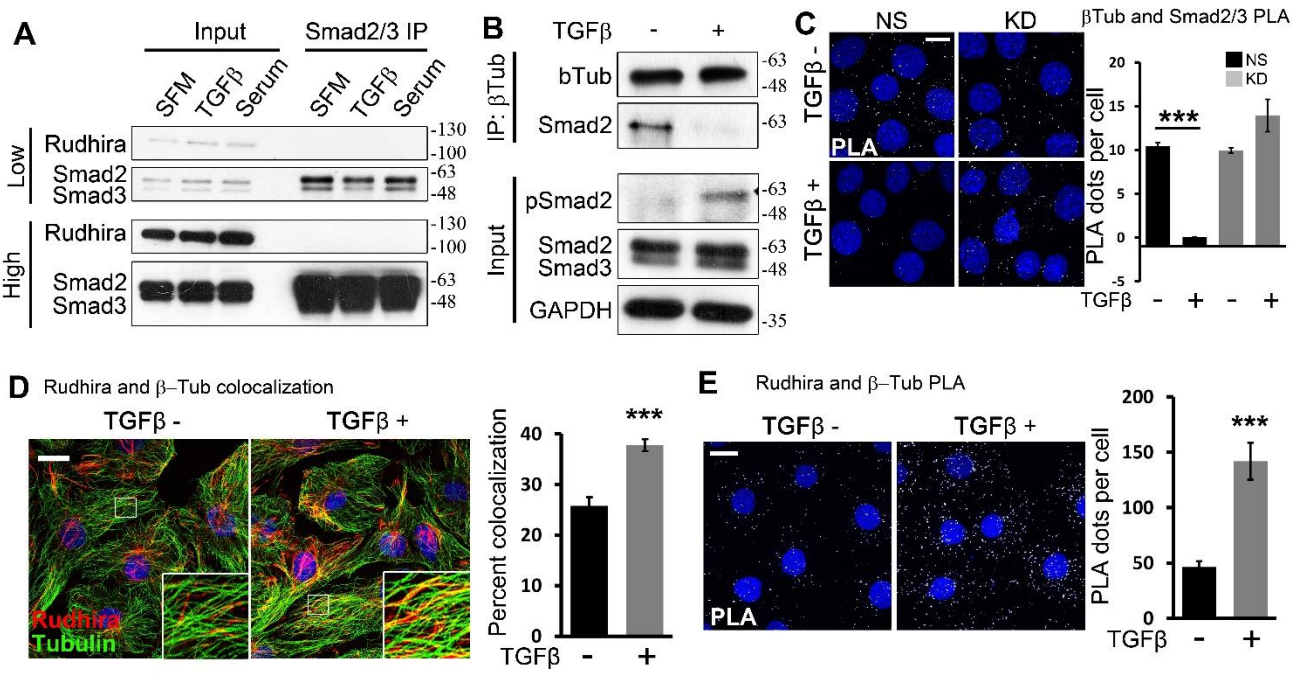


**Figure 3**

**Fig. 3. Rudhira is essential for the release of Smads from microtubules for TGFβ pathway activation.** (A) Analysis of interaction between Rudhira, Smad2/3 and MTs by co-immunoprecipitation and immunoblotting, as indicated (N= 3 independent experiments). (B) Loss of Smad-MT interaction on TGFβ stimulation in SVEC cells (N= 3 independent experiments). (C) NS and KD cells were analyzed for MT and Smad2/3 interaction by PLA for Tubulin and Smad2/3 with or without TGFβ treatment. PLA dots represent Smad2/3 and β-tubulin interaction. Graph shows the quantitation of PLA dots per cell (quantitation from >80 cells for two knockdown cell lines from N= 3 independent experiments; also see Fig. S3). (D, E) Association of Rudhira and MTs was analyzed by immunostaining (D) or Proximity Ligation Assay (PLA) (E) for Rudhira and Tubulin with or without TGFβ stimulation in SVEC. PLA dots represent Rudhira and β-tubulin interaction. Graph (D) shows the quantitation of colocalization percentage (quantitation from ~40 cells from 9 images each with or without TGFβ respectively from N= 3 independent experiments) and graph (E) shows the quantitation of PLA dots per cell (quantitation from 86 or 68 cells from 9 images each with or without TGFβ respectively from N= 3 independent experiments). Statistical analysis was performed using one-way ANOVA. Error bars indicate SEM. Scale bar: (C) 20 µm; (D, E) 10 µm. *p<0.05, **p<0.01, ***p<0.001.

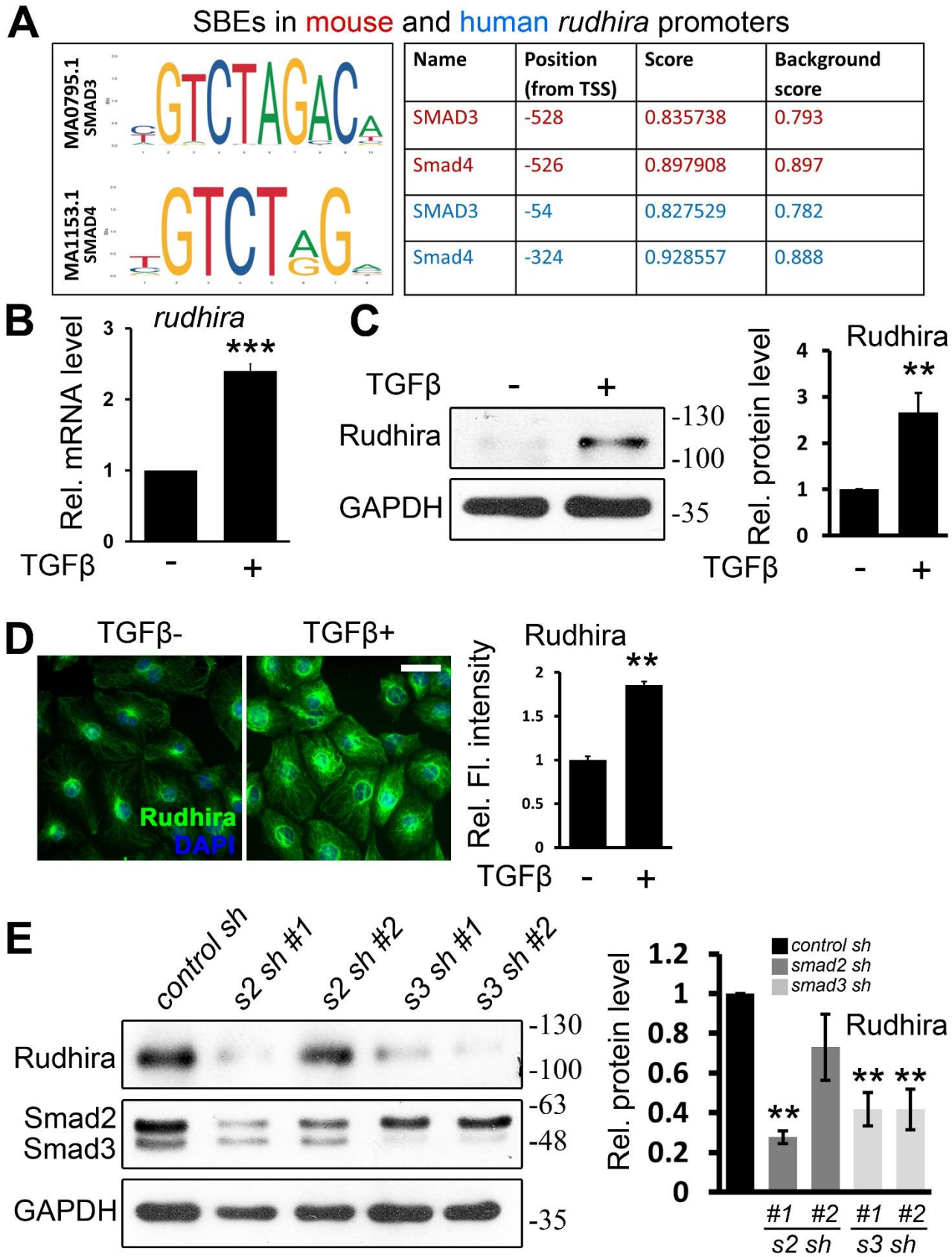
A
SBEs in mouse and human rudhira promoters
MA0795.1 SMAD3
MA1153.1 SMAD4
B
rudhira
Rel. mRNA level
***
TGFβ - +
C
TGFβ - +
Rudhira
GAPDH
-130
-100
-35
Rudhira
Rel. protein level
**
TGFβ - +
D
TGFβ-
TGFβ+
Rudhira
DAPI
Rudhira
Rel. Fl. intensity
**
TGFβ - +
E
control sh
s2 sh #1
s2 sh #2
s3 sh #1
s3 sh #2
Rudhira
Smad2
Smad3
GAPDH
-130
-100
-63
-48
-35
control sh
smad2 sh
smad3 sh
Rudhira
Rel. protein level
**
** **
#1 #2
s2 sh
#1 #2
s3 sh

**Figure 4**

516

517 **Fig. 4. Rudhira is a Smad2/3-dependent target of TGFβ signaling.** (A) Smad-binding element
518 (SBE) matrix (SMAD3, ID MA0795.1; Smad4, ID MA1153.1) and predicted binding sites in mouse
519 (in red) and human (in blue) *rudhira* promoters, from JASPAR and PSCAN bioinformatics tool. (B-
520 D) TGFβ stimulation followed by qRT-PCR (B), immunoblot (C) or immunostaining (D) analysis
521 (quantitation from 34 cells in each condition) of Rudhira levels in SVEC cells. Graphs in (C) and (D)
522 show the quantitation of Rudhira levels with or without TGFβ (N= 3 independent experiments). (E)
523 Analysis of Rudhira levels upon *smad2* or *smad3* knockdown in HEK293T cells by immunoblotting
524 (N= 3 independent experiments). Statistical analysis was performed using one-way ANOVA. Error
525 bars indicate SEM. Scale bar: (D) 10 µm. *p<0.05, **p<0.01, ***p<0.001.

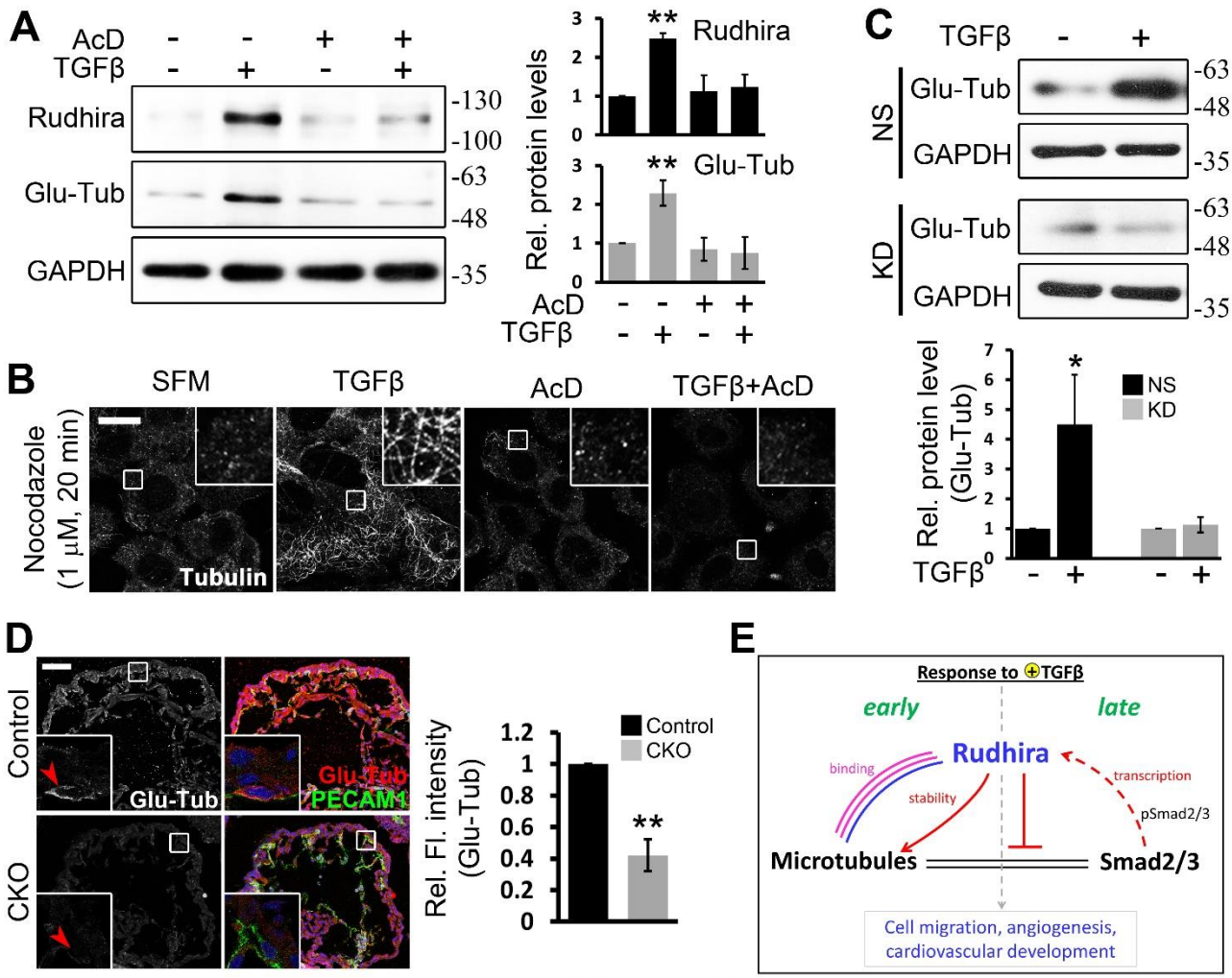


**Figure 5**

**Fig. 5. TGFβ-dependent *rudhira* transcription stabilizes MTs.** (A) Analysis of Rudhira levels and MT stability (marked by Glu-Tubulin) upon treatments as indicated, by immunoblotting. Graphs show the quantitation of Rudhira or Glu-Tub levels (N= 3 independent experiments). (B) Analysis of MT resistance to Nocodazole mediated depolymerization at indicated dosage and time (N= 30 cells). (C) MT stability in serum starved NS or KD SVEC cells kept untreated or treated with TGFβ was analyzed by immunoblot for Glu-Tubulin. Graph shows the quantitation of Glu-Tub levels (N= 3 independent experiments). (D) Immunostaining for Glu-Tubulin in control and *rudhira* conditional knockout *(rudh$^{CKO}$)* embryos at E10.5. Endocardium in the heart is marked by PECAM1. Boxed region in the embryonic heart is magnified in the insets. Red arrowheads in the insets mark the PECAM1 positive cells (N= 4 embryos for each genotype). Graph shows the quantitation of Glu-Tub fluorescence intensity in the endocardium. (E) Model depicting cellular and molecular response to

538 TGF addition. Rudhira has an early and a late effect on MTs. Previously known information
539 about Rudhira is shown in blue. Events identified in this study are shown in red or pink. Parallel
540 lines indicate protein- protein interaction. Solid lines indicate direct effects. Dotted lines indicate
541 effects that may be direct or indirect. Arrows indicate positive regulation. Bar-headed line
542 indicates inhibition. Statistical analysis was performed using one-way ANOVA. Error bars indicate
543 SEM. Scale bar: (B) 10 µm; (D) 100 µm. *p<0.05, **p<0.01, ***p<0.001.

544

545

546

547

548

549

550

**Rudhira-mediated microtubule stability controls TGFβ signaling during mouse vascular development.**

Divyesh Joshi[1#], Preeti Jindal[1#], Ronak Shetty[1] and Maneesha S. Inamdar[1,2*]

[1]Jawaharlal Nehru Centre for Advanced Scientific Research, Bangalore, India;[2]Institute for Stem Cell Science and Regenerative Medicine (inStem), Bangalore, India.

**Supplementary Figures and Figure legends**

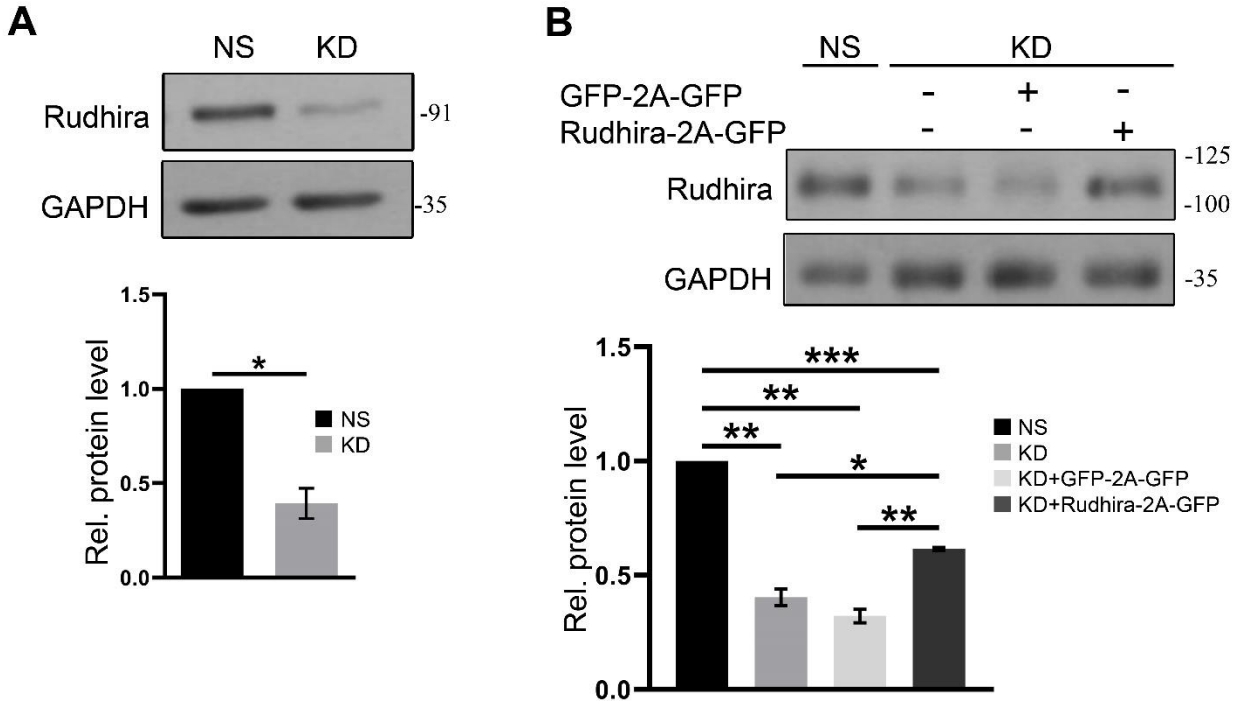


**Figure S1**

**Fig. S1 (related to Fig. 1). Cell line validation.** (A, B) Validation of Rudhira knockdown and restoration in SVEC cells by immunoblotting. Statistical analysis was performed using one-sample t-test. Error bars indicate standard error of mean (SEM). *p<0.05, **p<0.01,***p<0.001.

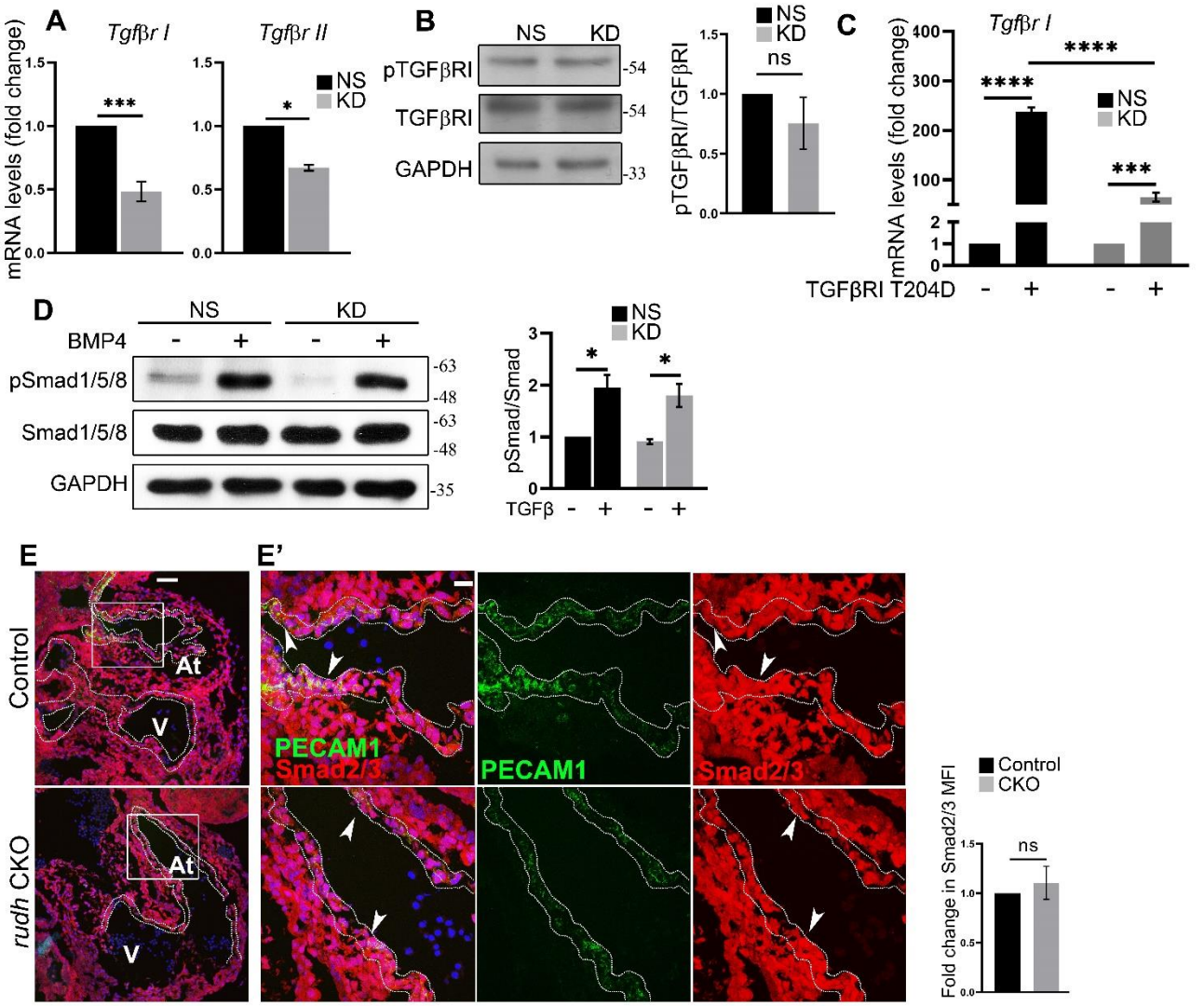


**Figure S2**

**Fig. S2 (related to Fig. 1). Rudhira acts downstream to TGFβ receptors.** (A) qRT-PCR analysis of *tgfβrI* and *tgfβrII* in Rudhira knockdown endothelial cells (N= 3 independent experiments). (B) TGFβRI phosphorylation was analyzed using immunoblot technique in SVEC NS and KD. Graph shows the quantitation of pTGFβRI/TGFβRI levels (N= 3 independent experiments). (C) NS and KD SVEC cells, transfected with constitutively active TGFβRI for 24h, were analyzed for total TGFβRI level by qRT-PCR. (D) SVEC control (NS) and knockdown (KD) cells were stimulated by BMP4 and used for immunoblotting of pSmad1/5/8. Graph shows the quantitation of pSmad1/5/8 by Smad1/5/8 levels (N= 3 independent experiments). (E, E') Immunostaining for total Smad2/3 in control and rudhira conditional knockout (rudhCKO) embryos at E10.5. Boxed region in the embryonic heart in (E) marking the endocardium and the myocardium are magnified in (E') (N= 3 embryos for each genotype). White dotted line indicates the endocardium. Graph shows the quantitation of Smad2/3 level (N= 3 independent experiments). Statistical analysis was performed using one-sample t-test.

Error bars indicate standard error of mean (SEM). *p<0.05, **p<0.01,***p<0.001, ****p<0.0001. Scale bar: (E) 100 µm; (E') 20 µm.

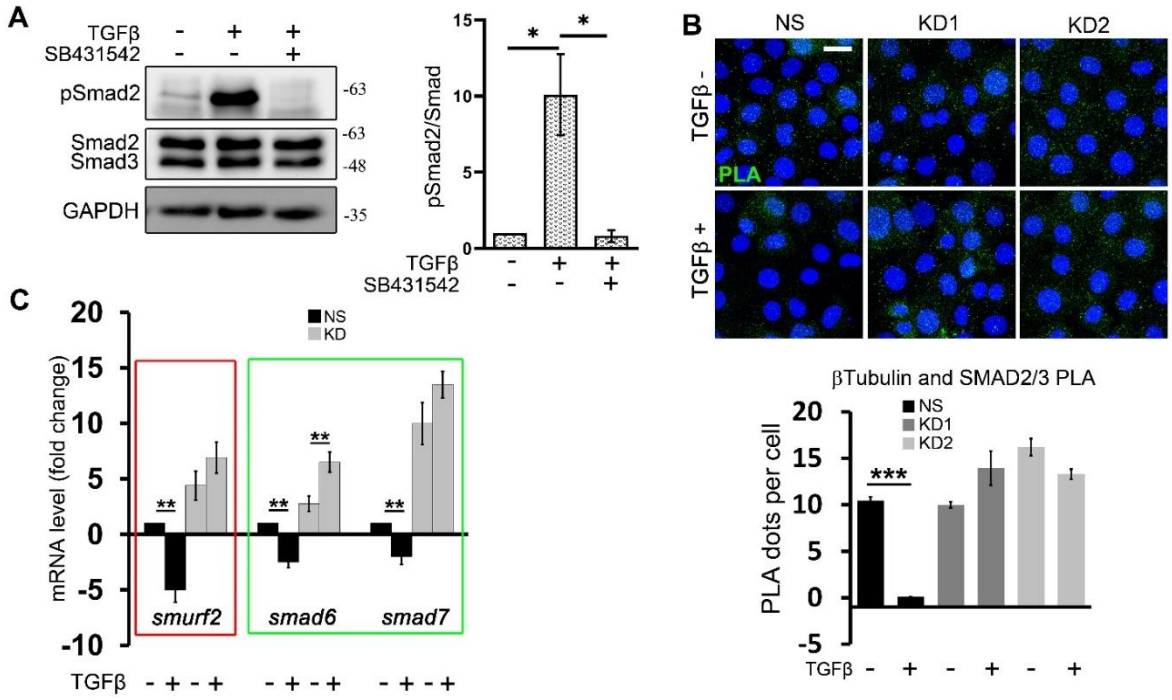


**Figure S3**

**Fig. S3 (related to Fig. 1, 2 and 3). Rudhira specifically regulates TGFβ-dependent Smad2/3 activation.** (A) SVEC cells treated with SB431542 (10µM) for 2h and analyzed for Smad2 phosphorylation by Immunoblotting. (B) NS and two KD SVEC lines (KD1 and KD2) were analyzed for MT-SMAD interaction by PLA for β-Tubulin and Smad2/3 With or without TGFβ treatment (N= 3 independent experiments). (C) qRT-PCR analysis of negative regulators of TGFβ pathway (N=3 independent experiments). Statistical analysis was performed Using One way ANOVA. Error bars indicate standard error of mean (SEM). Scale bar (B): 20 µm. *p<0.05, **p<0.01, ***p<0.001.

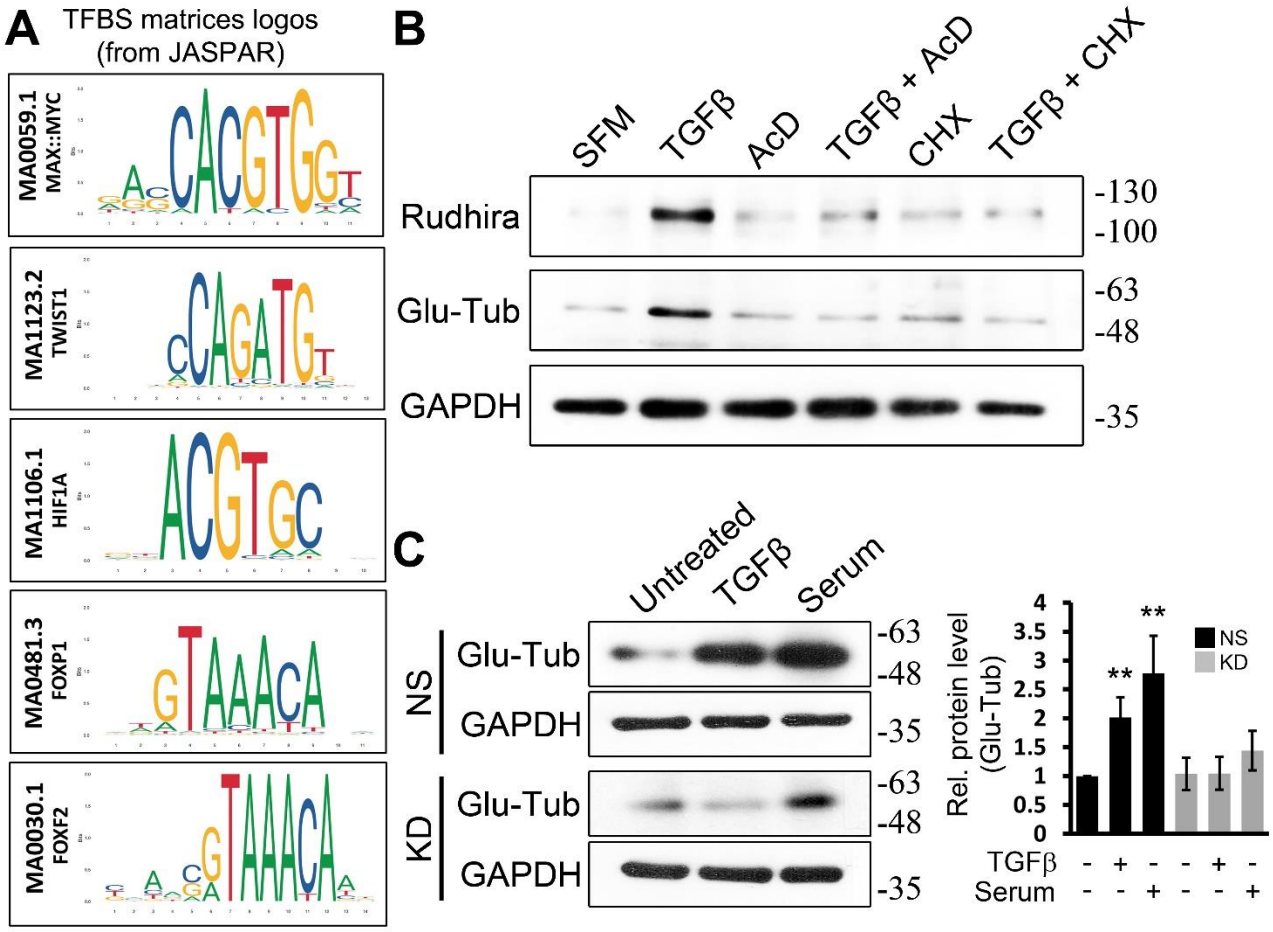


**Figure S4**

**Fig. S4 (related to Figs. 4 and 5). TGFβ induces *rudhira* transcription for MT stability.** (A) Transcription factor binding sites (TFBS) available from JASPAR and PSCAN bioinformatics tool(B) Analysis of Rudhira levels and MT stability (marked by Glu-Tubulin) upon treatments as indicated by immunoblotting (N= 3 independent experiments). (C) Analysis of MT stability in serum starved WT and KD cells kept untreated or treated with TGFβ or serum (N= 3 independent experiments).

46 **Supplementary Tables**

47 **Supplementary Table S1. Primers used for qRT-PCR analysis.**

48

| **Gene** | **Forward primer (5' to 3')** | **Reverse primer (5' to 3')** |
|---|---|---|
| *rudhira* | TCCTACATGGAGAGCGTCG | GGAGGCTCATTTCCAGTGC |
| *smurf2* | AGACTGGTGTGAGCACATGG | CTTCCTGTTGCGGTATTGCG |
| *smad6* | GGGTGAATTCTCAGACGCC | GGTCGTACACCGCATAGAGG |
| *smad7* | CGGAAGTCAAGAGGCTGTGT | GACAGCCTGCAGTTGGTTTG |
| *pai1* | CTGTGCCCATGATGGCTCAG | ATGAACATGCTGAGGGTGTC |
| *mmp9* | GTCCAGACCAAGGGTACAGC | ATACAGCGGGTACATGAGCG |
| *gapdh* | GGTGAGGCCGGTGCTGAG | TGATGTCATCATACTTGGCAGG |

49

50

51 **Supplementary Table S2. Predicted Transcription factor binding sites in mouse and human**

52 ***rudhira/BCAS3* promoters, obtained from JASPAR bioinformatics tool.**

53

| Name | Position (from TSS) | Score | Background score | p-value | Matrix ID (JASPAR) | Strand | Predicted sequence |
|---|---|---|---|---|---|---|---|
| MAX::MYC | -428 | 0.959466 | 0.823 | 0.00252271 | MA0059.1 | - | AAGCACGTGGA |
| MYC | -429 | 0.959143 | 0.827 | 0.00590903 | MA0147.3 | + | GTCCACGTGCTT |
| TWIST1 | -651 | 0.988341 | 0.854 | 0.00194672 | MA1123.2 | + | TTTCCAGATGTTC |
| HIF1A | -427 | 0.952744 | 0.849 | 0.0315803 | MA1106.1 | + | CCACGTGCTT |
| FOXP1 | -386 | 0.992493 | 0.876 | 0.0124319 | MA0481.3 | + | ATGTAAACACA |
| FOXF2 | -515 | 0.932307 | 0.826 | 0.0101525 | MA0030.1 | + | GGAAGGTAAACACA |
| MAX::MYC | -431 | 0.965445 | 0.823 | 0.00084454 | MA0059.1 | - | GAGCACGTGGA |
| MYC | -432 | 0.97587 | 0.831 | 0.00370719 | MA0147.3 | + | GTCCACGTGCTC |
| TWIST1 | -412 | 0.88988 | 0.849 | 0.19157 | MA1123.2 | + | GAACCAGCTGTCG |
| HIF1A | -430 | 0.963428 | 0.856 | 0.0274206 | MA1106.1 | + | CCACGTGCTC |
| FOXP1 | -389 | 0.989613 | 0.864 | 0.0168508 | MA0481.3 | + | ATGTAAACAGA |
| FOXF2 | -518 | 0.932307 | 0.817 | 0.0116588 | MA0030.1 | + | GGAAGGTAAACACA |

54

55

56 **Supplementary Table S3. The oligonucleotide sequence of the *smad2* and *smad3* shRNAs.**

57

| **Gene target** | **Oligonucleotide sequence in the shRNA (target sequence in red)** |
|---|---|
| *Smad2 sh#1* | CCGGCGATTAGATGAGCTTGAGAAACTCGAGTTTCTCAAGCTCATCTAATCGTTTTTG |
| *Smad2 sh#2* | CCGGCCTAAGTGATAGTGCAATCTTCTCGAGAAGATTGCACTATCACTTAGGTTTTTG |
| *Smad3 sh#1* | CCGGGCCTCAGTGACAGCGCTATTTCTCGAGAAATAGCGCTGTCACTGAGGCTTTTTG |
| *Smad3 sh#2* | CCGGGAGCCTGGTCAAGAAACTCAACTCGAGTTGAGTTTCTTGACCAGGCTCTTTTTG |

58